Polarization Dependence of Palladium Deposition on Ferroelectric Lithium Niobate (0001) Surfaces

Seungchul Kim, Michael Rutenberg Schoenberg, and Andrew M. Rappe

Polarization-dependence of palladium deposition on ferroelectric lithium niobate (0001) surfaces

Seungchul Kim, Michael Rutenberg Schoenberg, and Andrew M. Rappe*
The Makineni Theoretical Laboratories, Department of Chemistry,
University of Pennsylvania, Philadelphia, Pennsylvania 19104–6323, USA
(Dated: June 20, 2011)

We investigate the effect of ferroelectric polarization direction on the geometric properties of Pd deposited on the positive and negative surfaces of LiNbO$_3$ (0001). We predict preferred geometries and diffusion properties of small Pd clusters using density functional theory, and use these calculations as the basis for kinetic Monte Carlo simulations of Pd deposition on a larger scale. Our results show that on the positive surface, Pd atoms favor a clustered configuration, while on the negative surface, Pd atoms are adsorbed in a more dispersed pattern due to suppression of diffusion and agglomeration. This suggests that the effect of LiNbO$_3$ polarization direction on the catalytic activity of Pd [J. Phys. Chem. **88**, 1148 (1984)] is due, at least in part, to differences in adsorption geometry. Further investigations using these methods can aid the search for catalysts whose activities switch reversibly with the polarization of their ferroelectric substrates.

The spontaneous polarization of ferroelectric materials has enabled their use in technological devices ranging from SONAR to random access memory. While most current applications of ferroelectrics result primarily from their bulk properties, polarization can also impact the surface properties of these materials, including surface stoichiometry [1–3], geometry [2, 3], and electronic structure [1, 3–5]. These polarization dependent differences in intrinsic surface properties also affect their interactions with adsorbates, [6–13] as evidenced by differences in adsorption energies [6–10] or the rates of surface catalyzed reactions [11–13]. Polarization orientation can, in turn, affect the chemical properties of the adsorbates themselves. For example, Inoue *et al.* [11] showed that the activation barrier for CO oxidation by Pd adsorbed on a LiNbO$_3$ surface changes by 30 kJ/mol, depending on polarization orientation. The notion that a ferroelectric substrate's polarization can affect the activity of a supported catalyst suggests the intriguing possibility that the activity of a catalyst could be modulated reversibly by switching the polarization of a ferroelectric substrate.

Despite ample evidence showing that metals on oppositely poled ferroelectric surfaces have different catalytic properties, the mechanism underlying these differences is not well understood. The most prevalent explanation for this phenomenon has been that the difference in charge between the two surfaces alters the electronic properties of the catalyst [4, 11–13]. However, this explanation may be incomplete, as metal adsorption geometries significantly impact their catalytic properties [14]. Since ferroelectric surfaces may have different geometries depending on the sign of their polarization [1–3], it is plausible that the geometries of metals adsorbed onto them also differ [10, 15]. Two recent studies of Pd adsorption on oppositely poled LiNbO$_3$ (0001) surfaces present conflicting conclusions regarding the possible effect of polarization on metal adsorption geometry. Yun *et al.* [15] showed that large Pd clusters form on both the positive (c^+) and negative (c^-) surfaces of LiNbO$_3$, suggesting that polarization has little impact on metal adsorption geometry. In contrast, Zhao *et al.* [10] observed large Pd clusters only on the c^+ surface, and a more planar geometry on the c^- surface, suggesting that polarization strongly affects metal adsorption geometry. In addition, only Zhao *et al.* observed a difference in CO temperature programmed deposition between the two surfaces, suggesting that when polarization affects the activity of adsorbed catalysts, it does so, at least in part, by altering their geometries.

In view of the ambiguity of experimental investigations of the relationship between polarization and metal adsorption geometry, we address this question on a microscopic level using theoretical methods. Here we investigate the energetics and kinetics of Pd deposition on LiNbO$_3$ (0001) surfaces using a combination of density functional theory (DFT) calculations and kinetic Monte Carlo (KMC) simulations. We first calculate the adsorption geometries of clusters on the c^+ and c^- surfaces. We then model the range of possible diffusion and agglomeration processes of these clusters using the nudged elastic band (NEB) method [16]. Finally, we use the activation barriers of these processes as inputs for a KMC simulation of the deposition of Pd on LiNbO$_3$ on a larger scale. To our knowledge, this is the first theoretical study of metal adsorption kinetics on a ferroelectric surface.

In all DFT calculations, we studied five trilayer thick LiNbO$_3$ slabs with $\sqrt{3} \times \sqrt{3}$ surface supercells (Supplementary Fig. S1). We passivated surface charges with one Li atom per primitive supercell on the c^+ surface, and one O and one Li atom on c^-, in accordance with the findings of Levchenko and Rappe that this is the most thermodynamically stable surface composition for
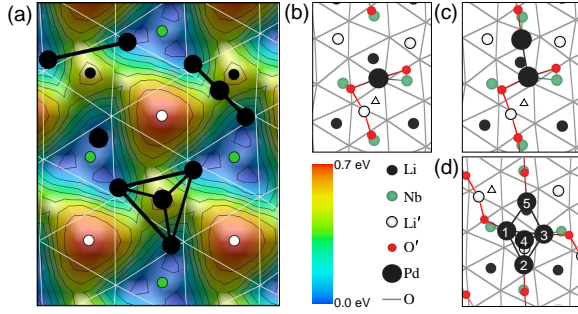
FIG. 1: (Color online) (a) Left Side: Monomeric potential energy surface and minimum energy geometries of Pd_1, Pd_2, Pd_3 and Pd_4 on c^+. Contour spacing is 0.1 eV. Right side: Minimum energy geometries of (b) Pd_1, (c) Pd_2, and (d) Pd_5 on c^-. Triangles are original positions of Li′. The geometries for Pd_3 and Pd_4 are similar to those of atoms 1-2-3 and 1-2-3-4 in (d).

LiNbO$_3$ [2]. Hereafter, we denote these passivation atoms as Li′ and O′. DFT total energy calculations [17] were performed using the generalized gradient approximation (GGA-PBE) [18] and implemented using the Quantum ESPRESSO [19]. Atoms were represented using norm-conserving nonlocal pseudopotentials [20, 21] generated using the OPIUM code [22].

Our DFT results for Pd adsorption show differences in preferred binding geometries and diffusion barriers between the c^+ and c^- surfaces. On the c^+ surface, Pd adsorption minimally changes the geometry of the LiNbO$_3$ surface itself. As a result, the monomeric potential energy surface (PES, Fig. 1(a)) essentially determines the geometries of multiple Pd atoms adsorbed on this surface. In particular, all Pd atoms that we predict to bind directly to the c^+ surface prefer sites close to monomeric potential energy minima. However, because the distances between minima do not match well with optimal Pd-Pd bond lengths, binding of large numbers of Pd atoms both to the c^+ surface and to each other is unfavorable. For example, adsorption geometries of three and four Pd atoms both include one atom that bonds only to other Pd atoms and does not interact directly with the surface (Fig. 1(a)). Further, we found no metastable planar structure of four atoms, suggesting that the Pd agglomeration barrier on the c^+ surface is negligible.

Diffusion and agglomeration processes on the c^+ surface are also impacted by the monomeric PES. In the monomeric case, this relationship is direct, as the two unique paths for monomer hopping (Fig. 2(a)) are the only paths containing saddle points on the PES. Because the diffusion processes of clusters of up to four atoms on the c^+ surface are dominated by the movement of a single atom, they have diffusion barriers similar to monomer hopping, a fact that can also be explained by the monomeric PES. For example, in dimer walking, a process in which one atom in a dimer steps between

two potential minima and stays bonded to the other Pd, paths 2 and 3 have activation barriers similar to monomer hopping paths 1 and 2, respectively (Fig. 2(b)). Similarly, though dimer sliding involves movement of both Pd atoms, one stays adjacent to the same Nb atom and thus, its movement contributes little to the activation barrier (Fig. 2(c)). Finally, because tetramer rolling requires movement of only one Pd atom out of a monomeric potential well, it too has an activation barrier similar to that of monomer hopping. The combination of low Pd diffusion barriers and a negligible agglomeration barrier suggests that formation of large Pd clusters is favorable on the c^+ surface.

In contrast to its behavior on the c^+ surface, Pd adsorption on the c^- surface substantially alters the geometry of the surface itself. This is largely due to interactions with O′ atoms, which along with Li′ atoms terminate the c^- surface for charge passivation [2]. The formation of Pd-O′ bonds makes adsorption onto the c^- surface much more favorable than on c^+ (Supplementary Table S1). However this also leads to complex adsorption geometries, as the O′ atom is free to tilt its bond to Nb substantially in order to accommodate bonding to Pd. Despite this geometric complexity, we find that the Pd adsorption geometries on the c^- surface can be understood in the context of maximizing the number of Pd-Pd and Pd-O′ bonds formed. For example, this explains why the 2D planar (not shown) and 3D configurations of clusters of four or five Pd atoms on the c^- surface, which have identical numbers of Pd-Pd/Pd-O′ bonds, have binding energies within 0.1 eV of one another.

The inherent assumption in this analysis, that Pd-O′ and Pd-Pd bonds have similar strengths, is justified by two facts. First, the average energies of these bonds, defined as adsorption energies divided by the number of Pd-Pd and Pd-O′ bonds, in clusters of 1–5 Pd atoms are uniform (1.03 ± 0.05 eV). Second, these average bond energy values are similar to bond strengths in free clusters of 2–5 Pd atoms (1.06 ± 0.08 eV). From here on, we denote Pd-Pd and Pd-O′ bonds as Pd-X.

Just as Pd-X bonds are the primary contributors to the favorable adsorption energy of Pd clusters on the c^- surface, breaking these bonds, particularly Pd-O′, is the primary barrier to cluster diffusion and agglomeration. Based on the argument above that Pd-X bonds have similar energies, we would expect the activation barriers for processes that require one Pd-O′ bond breaking to be approximately 1 eV. However, actual activation barriers are lower, because other atoms can move to more favorable positions in the process of transition state formation. This is especially true when new Pd-X bonds are formed before a Pd-X bond is fully broken. Consistent with our understanding of the effect of Pd-X bond breaking on the activation barriers of diffusion processes, we find that in-plane movement at the boundary of a cluster has a high activation barrier (path 2 in Fig. 2(h)), because it re-
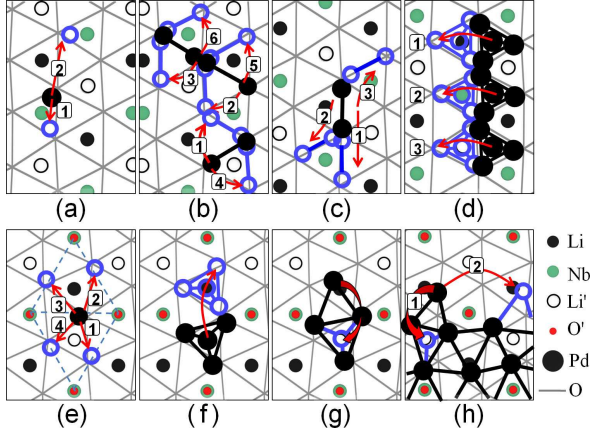
FIG. 2: (Color online) Schematic drawings of kinetic events. Top: Diffusion events on c^+. (a) Pd_1 hopping, (b) Pd_2 walking, (c) Pd_2 sliding and (d) Pd_4 rolling. Bottom: Diffusion events on c^-. (e) Pd_1 hopping, (f) Pd_4 rolling, (g) Pd_4 agglomeration, and (h) agglomeration at large cluster (path 1) and in-plane motion (path 2). Large black circles and open blue circles denote initial and final positions for events. after the events. Blue dashed lines in (e) indicate that Pd_1 hops between O' bridge sites. In many cases, these events involve traversing barriers and visiting metastable local minima.

	path	1	2	3	4	5	6
c^+	Pd_1 hopping	0.09	0.39				
	Pd_2 walking	0.26	0.12	0.38	0.24	0.38	0.17
		0.32	0.02	0.41	0.24	0.38	0.17
	Pd_2 sliding	0.35	0.36	0.30			
		0.32	0.33	0.27			
	Pd_3 walking	0.23	0.19	0.27	0.24	0.11	0.18
		0.12	0.11	0.46	0.24	0.11	0.18
	Pd_4 rolling	<0.01	0.21	0.06			
		0.40	0.14	0.13			
	Pd_2 dissociation	0.55					
c^-	Pd_1 hopping	0.82	0.87	0.87	0.82		
	Pd_2 sliding	1.06					
	Pd_3 flipping (Li' →Li)	1.30	(1.31)				
	Pd_4 rolling (Li' →Li)	0.85	(0.70)				
	Pd_2 dissociation	0.77					
	large cluster, in-plane	1.12					
	large cluster, agglom.	0.74	(0.93)				
	Pd_4, agglom.	0.59	(0.61)				

TABLE I: Diffusion activation barriers (in eV) of processes drawn in Fig. 2 and described in the text. Barriers of reverse processes are written below forward processes (c^+) or in parentheses (c^-).

quires breaking of two Pd-X bonds.

Despite the fact that the c^+ and c^- surface are oppositely poled, our electronic structure calculations show that the Pd-LNO bonds formed on both surfaces have very similar electronic and structural characteristics (Fig. S2). This indicates that the kinetic differences between the two surfaces are primarily geometric in origin, and depend mainly on the number of Pd-O bonds formed, rather than on electronic considerations such as the charge of the polar surface.

Our DFT calculations show that diffusion barriers are substantially lower on the c^+ surface ($\lesssim 0.4$ eV) than on the c^- surface ($\gtrsim 0.8$ eV). These activation energies, E_a, can be compared in a physically meaningful way when converted to expected event-event time intervals, τ, using Arrhenius kinetics [23], $\frac{1}{\tau} = \nu e^{-E_a/k_B T}$. Assuming an attempt frequency ($\nu = 10^{12}$ sec^{-1} [24]) the time scales of diffusion events on the c^+ and c^- surfaces are on the order of microseconds and minutes, respectively, at 300 K. We can then infer that at a deposition rate of ≈ 0.01–0.1 ML/s [15], on average, each new monomer deposited on c^+ will aggregate to an existing cluster before the next atom is deposited. In contrast, we would expect many Pd atoms to be deposited in the vicinity of a given Pd atom on c^- between diffusion events of that atom. Although we find that cluster formation is thermodynamically favorable on both surfaces (Table S1), we infer that the much larger kinetic barrier to diffusion on c^- leads to Pd atom agglomeration into large clusters on the c^+ surface and wetting or tiny clusters on c^-.

We conducted kinetic Monte Carlo (KMC) simulations

in order to characterize this inferred difference in adsorption geometries. Onto a 10 nm × 10 nm surface, we randomly deposited Pd atoms one by one at a selected deposition rate. We then allowed Pd atoms and clusters to attempt a series of diffusion and agglomeration processes, with probabilities based on our calculated activation barriers, at a constant attempt frequency of 10^{12} sec^{-1} [25] for all events (Full KMC description in Supplement).

Our KMC simulations confirm that Pd forms larger clusters on the c^+ surface than on the c^- surface. Correspondingly, we find that Pd covers a much smaller area of the c^+ surface than of c^-. We also find that Pd area is insensitive to deposition rate at room temperature (Fig. 3 (a)), as all processes are highly activated (for c^+) or suppressed (for c^-) at this temperature. Changing the deposition rate strongly affects the geometry only when it is near the (T-dependent) diffusion time scale. Please see the supplement (Fig. S4) for a graphical representation of how temperature and deposition rate translate to Pd morphology on the two LiNbO$_3$ terminations, for a wide range of conditions.

The relatively large diffusion barriers on the c^- surface (≈ 0.8 eV) were not sufficient to prevent agglomeration completely, especially when our simulations were extended until slightly after deposition was complete. However, we infer that the clusters on the c^- surface remain much smaller than those on the c^+ surface over a very long time scale (Supplementary Fig. S3).
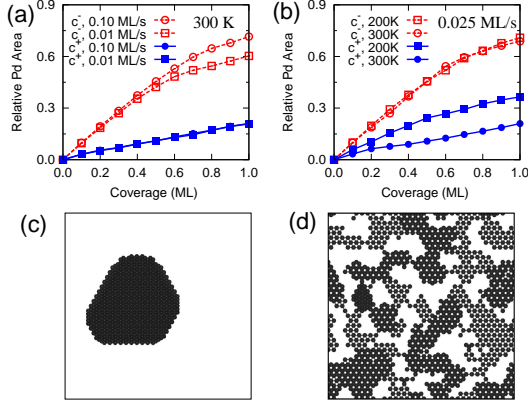
FIG. 3: (Color online) Proportion of surface area covered by Pd for simulations at a range of (a) deposition rates at 300 K and (b) temperatures with a deposition rate of 0.025 ML/s. KMC snapshots of 1.0 ML on (c) c^+ and (d) c^- at 300 K with a 0.025 ML/s deposition rate.

Overall, our results support the conclusion of Zhao *et al.* that Pd cluster sizes are much larger on the c^+ surface than on c^- [10]. However, Yun *et al.* also produced a thorough data set supporting their conclusion that Pd forms large clusters on both surfaces of $LiNbO_3$ [15]. One possible explanation is that Yun and Zhao studied Pd adsorption onto $LiNbO_3$ surfaces with substantially different compositions. This could be due to the presence of different impurities, such as hydroxyl groups [26], which are known to exist on some $LiNbO_3$ surfaces, or oxygen lattice vacancies [3]. Our calculations predict that Pd binding is weaker by 0.6 eV to a c^- surface terminated with OH instead of OLi, suggesting that agglomeration would be more favorable with some OH impurities present. Thus, it is plausible that if there were OH impurities on the c^- surface studied by Yun *et al.*, they may have influenced the formation of larger Pd clusters.

In conclusion, we find that the different surface geometries of oppositely poled $LiNbO_3$ (0001) surfaces lead to substantially different Pd adsorption geometries. On the c^- surface, strong Pd bonding to O', the extra surface oxygen present for charge passivation, leads to larger diffusion and agglomeration barriers. This lead in turn to less clustering and a more dispersed geometry on this surface than on c^+. In contrast to the prevalent view that differences in catalyst charging are responsible for differences in the catalytic properties of metals adsorbed on polar ferroelectric surfaces, we conclude that the difference in adsorption geometry predicted here is sufficient to explain much of the difference in catalytic activity that has been observed for Pd deposited on oppositely poled $LiNbO_3$ surfaces [11]. Because formation of large Pd clusters is thermodynamically favorable on both c^+ and c^-, it is unlikely that the catalytic activity of Pd could be switched reversibly by switching the polarization of the $LiNbO_3$ substrate. However, the combination of theoreti-

cal methods used here is well suited for the study of other metal/ferroelectric surface combinations in search of systems with switchable catalytic activity, and the present example serves as a paradigm of polarization controlling catalytic cluster geometry and reactivity.

* corresponding author: rappe@sas.upenn.edu

[1] C. Noguera, J. Phys.: Condens. Matter **12**, R367 (2000).

[2] S. V. Levchenko and A. M. Rappe, Phys. Rev. Lett. **100**, 256101 (2008).

[3] Y. Yun, et al., Surf. Sci. **601**, 4636 (2007).

[4] Y. Inoue, K. Sato, and S. Suzuki, J. Phys. Chem. **89**, 2827 (1985).

[5] C. Park and R. T. K. Baker, J. Phys. Chem. B **104**, 4418 (2000).

[6] Y. Yun and E. I. Altman, J. Am. Chem. Soc. **129**, 15684 (2007).

[7] Y. Yun, et al., J. Phys. Chem. C **111**, 13951 (2007).

[8] A. M. Kolpak, I. Grinberg, and A. M. Rappe, Phys. Rev. Lett. **98**, 166101 (2007).

[9] D. Li, et al., Nature Mater. **7**, 473 (2008).

[10] M. S. H. Zhao, D. A. Bonnell, and J. M. Vohs, J. Vac. Sci. Technol. **27**, 1337 (2009).

[11] Y. Inoue, I. Yoshioka, and K. Sato, J. Phys. Chem. **88**, 1148 (1984).

[12] Y. Inoue, M. Matsukawa, and K. Sato, J. Physs. Chem. **96**, 2222 (1992).

[13] N. Saito, Y. Yukawa, and Y. Inoue, J. Phys. Chem. B **106**, 10179 (2002).

[14] J. K. Nørskov, et al., Chem. Soc. Rev. **37**, 2163 (2008).

[15] Y. Yun, et al., Surf. Sci. **603**, 3145 (2009).

[16] G. Henkelman, B. P. Uberuaga, and H. Jónsson, J. Chem. Phys. **113**, 9901 (2000).

[17] J. Ihm, A. Zunger, and M. L. Cohen, J. Phys. C **12**, 4409 (1979).

[18] J. P. Perdew, K. Burke, and M. Ernzerhof, Phys. Rev. Lett. **77**, 3865 (1996).

[19] P. Giannozzi, et al., J. Phys.:Condens. Matter **21**, 395502 (2009).

[20] A. M. Rappe, et al., Phys. Rev. B Rapid Comm. **41**, 1227 (1990).

[21] N. J. Ramer and A. M. Rappe, Phys. Rev. B **59**, 12471 (1999).

[22] http://opium.sourceforge.net.

[23] H. Brune, Surface Science Reports **31**, 121 (1998).

[24] L. Xu, et al., Surf. Sci. **600**, 1351 (2006).

[25] L. Xu, et al., Surf. Sci. **601**, 3133 (2007).

[26] T. Volk and M. Wöhlecke, *Lithium Niobate: Defects, Photorefraction and Ferroelectric Switching* (Springer, 2008).